Journal of Materials Chemistry A

Accepted Manuscript

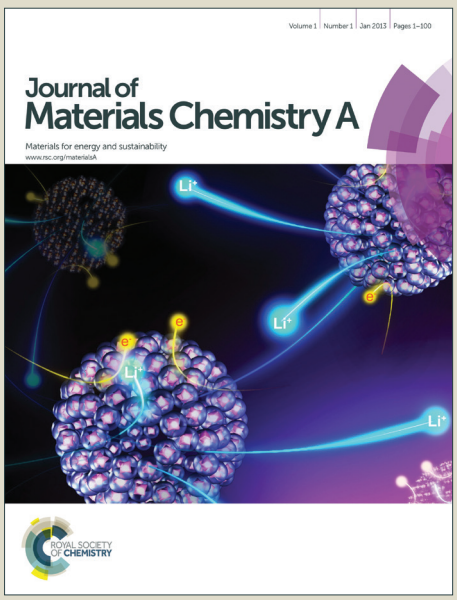

ROYAL SOCIETY OF CHEMISTRY

www.rsc.org/materialsA

J. Mater. Chem. A

RSCPublishing

ARTICLE

Composite of porous Co_3O_4 grown on Li_2MnO_3 microsphere as cathode material for lithium ion battery

Cite this: DOI: 10.1039/xOxx00000x

Received xx xxx 2014,
Accepted xx xxx 2014

DOI: 10.1039/xOxx00000x

www.rsc.org/

Faxing Wang[a,b], Zheng Chang [b], Xiaowei Wang [b], Yanfang Wang [b], Binwei Chen [b], Yusong Zhu[a,*] and Yuping Wu[a,b]*

The core-shell structure of Co_3O_4@Li_2MnO_3 was prepared by a facile hydrothermal method following a heat-treatment at 300 °C. The outer shell is porous and makes the diffusion of Li^+ ions to the inner shell easier. The synergetic effect between the core and shell shows that the Co_3O_4 shell in the composite serves as a host to react with lithium oxide removed from the Li_2MnO_3 core during the initial charging process, which eliminates the huge irreversible capacity loss of Li_2MnO_3. The composite as the cathode material for lithium ion batteries exhibits an attractive discharge capacity of 178 mAh g^{-1} with little irreversible capacity loss in the voltage range of 2.0-4.8 V. Its cycling performance is stable without any drastic capacity fading when cycling in the high voltage range of 2.0 – 4.6 V.

1. Introduction

The ever increasing demand in energy storage has stimulated significant interest in lithium ion battery. Lithium ion battery is one of the most promising systems due to its evident advantages over other rechargeable batteries in term of energy density and cycling life. Now lithium ion batteries are dominating the market of portable electronic devices.[1] To expand the use of lithium ion batteries, for instance as the onboard energy storage for electric vehicles (EVs), the specific energy density has to be increased. In order to arrive at this goal, it is necessary to increase the specific capacity and the tap density of those cathode materials. As well-known, the particle morphology is a very important factor affecting the density of materials, and materials composed of spherical particles have higher tap density than those of irregular particles. Recently, there have been some reports on spherical particles of battery electrode materials showing high tap densities, including $LiMn_2O_4$, [2a] $LiMn_{0.5}Fe_{0.5}PO_4$, [2b] $Li_4Ti_5O_{12}$, [2c] and hard carbon.[2d]

At the same time, to surpass the limitations associated with single phased materials, various composites have been proposed since some strong synergetic effect can be achieved by integrating functions of each individual component, hence realizing the full potential of the composite materials. Among them, core-shell structured materials have attracted special attention for energy storage systems. [3-5] For example, a core-shell structured SiO_x@Si composite as the anode for lithium ion battery successfully addressed the SEI stability issues and presented 6, 000 cycles with 88% capacity retention. [3b] The core-shell structured $LiFePO_4$@$LiMn_{0.85}Fe_{0.25}PO_4$ composite as the cathode has shown specific discharge capacity approaching the theoretical limit, stable cyclability even at 60 °C and exceptionally high tap density.[3e] Tin-core/carbon-sheath coaxial nanocables with uniform diameter and high aspect ratio exhibit high reversible specific capacities and remarkable high-rate capabilities.[4c] In our previous works, the core-shell structured PPy@MoO_3 and PPy@V_2O_5 resolve two problems of the host electrodes (poor electronic conductivity and high dissolution in liquid electrolytes).[5a,5b] However, all the above core-shell materials, as the cathode or anode for lithium ion battery, ignore an important issue: how can Li^+ ions easily reach the surface of host materials (core) through the compact outer shell. The thick shell (> 5 nm) may elongate the pathway for lithium ion diffusion through the stacked coating, which affects the lithium ion diffusivity.

Li_2MnO_3, which can be rewritten as $Li[Li_{1/3}Mn_{2/3}]O_2$ with C2/m space group symmetry, is known to be electrochemically inactive material because of the presence of Mn in its +4 valence. However, it can be made as electrochemically active cathode material by extracting Li and oxygen (or lithium oxide) from the structure either by chemical or electrochemical means.[6-12] The ideal capacity of Li_2MnO_3 could reach 459 mAh g^{-1} upon total Li deintercalation. Its reversible capacity is highly dependent on the morphology. For example, the Li_2MnO_3 micro-particles only show a discharge capacity of less 50 mAh g^{-1}.[10d] The Li_2MnO_3 nanoparticles could deliver a discharge capacity of 250 mAh g^{-1}.[10a] However, due to the removal of oxygen above 4.5 V, it suffers from a huge

irreversible capacity loss, which can be above 130 mAh g^{-1}. Most seriously, the emission of O_2 in the organic electrolyte is very dangerous and easily causes the safety issue.

In this paper, Li_2MnO_3 microsphere was synthesized by a simple solid-state reaction. Then a core-shell structure of porous Co_3O_4 grown on Li_2MnO_3 microsphere was prepared by simple hydrothermal method following with a heat-treatment. Since the outer shell Co_3O_4 is porous, the Li ions can easily pass through the outer shell and intercalate/de-intercalate into/from the core. More importantly, the Co_3O_4 in the outer shell successfully solves the irreversible capacity loss and the oxygen emission of Li_2MnO_3 since the Co_3O_4 shell in the composite can serve as a host to react with lithium oxide and produce electrochemically active Li_xCoO_y which can provide available lithium ions for the intercalation. This is quite different from previous reported surface modifications of solid solutions of Li_2MnO_3 with $LiMO_2$ (M = Mn, Co, Ni) by inactive oxides such as ZrO_2, AlF_3 and $AlPO_4$.[13-17] In our case, the "synergistic effect" between the core (Li_2MnO_3 microspheres) and shell (porous Co_3O_4), for the first time, eliminate the oxygen emission and decrease initial irreversible capacity of Li_2MnO_3 cathode materials.

2. Experimental

Samples preparation

The $MnCO_3$ microspheres were prepared by a precipitation method. [18a] In brief, $MnSO_4 \cdot H_2O$ (1.69 g) was dissolved in 700 ml distilled water. $NaHCO_3$ (8.4 g) was dissolved in another 700 ml distilled water. Ethanol (70 mL) and the $NaHCO_3$ solution were then added to the $MnSO_4 \cdot H_2O$ solution in sequence under stirring. The mixture was kept under stirring for 3 hour at 25 ^oC and then centrifuged, washed with water and ethanol for three times, respectively. After drying at 80 ^oC, the as-prepared $MnCO_3$ was added into LiOH solution (molar ratio of Li : Mn = 1:2), and sonicated about 1 h. Then the mixture was dried at 100 ^oC, and transferred into a furnace and heat-treated at 500 ^oC for 15 h to get Li_2MnO_3 microspheres. To prepare core-shell Co_3O_4@Li_2MnO_3, 0.25g $Co(CH_3COO)_2 \cdot 4H_2O$ was added into 30 mL 0.65 mol l^{-1} ammonia solution, then sonicated about 0.5 h. Later, 0.25 g as-prepared Li_2MnO_3 microspheres were immersed into the above solution by ultrasonication for another 0.5 h. This mixture was then transferred into a 50 mL autoclave, which was sealed and maintained at 150 ^oC for 5 h. The resulting products were separated by centrifugation, washed with deionized water, dried at 60 ^oC for 5 h, and then heat-treated in air at 300 ^oC for 1 h. The rising rate of temperature was 1 ^oC min^{-1}. All chemicals were of analytical grade, and the aqueous solutions were prepared with distilled water.

Material characterization

X-ray diffraction (XRD) patterns were collected using a BrukerD4 X-ray diffractometer (Bruker, Germany) with Ni-filtered Cu Karadiation (40 kV, 40 mA). Scanning electron micrographs (SEM) were obtained with a Philip XL30 microscope (Philips, The Netherlands) operated at 25 kV. Field emission scanning electron micrographs (FESEM) were obtained with a FE-SEM-4800-1. Prior to measurement of SEM and FESEM, a thin layer of Au was sputtered on the surface of the as-prepared materials. Transmission electron micrographs (TEM) were acquired using a JEOL JEM-2010 transmission electron microscope (JEOL, Japan) operated at 200 kV. Samples were first dispersed in ethanol and then collected using carbon-film-covered copper grids for TEM analysis. Nitrogen sorption-desorption isotherms were measured at 77 K with a Micromeritics Tristar 3000 analyzer (Micromeritics, U.S.A.). Prior to the measurements, the samples were degassed in vacuum at 200 ^oC for 10 h. The Brunauere Emmette Teller (BET) method was utilized to calculate the specific surface areas (S_{BET}). Using the Barrett Joyner Halenda (BJH) model, the pore volumes and size distributions were derived from the adsorption branches of the isotherms, and the total pore volumes were estimated from the adsorbed amount at a relative pressure P/P_0 of 0.995. Surface electronic states were investigated by X-ray photoelectron spectroscopy (XPS; Perkin-Elmer PHI 5000C ESCA, using Al KR radiation) and the binding energy values were calibrated by using C_{1s} of graphite at 284.6 eV as a reference. Both electrodes were taken out of the batteries and rinsed with anhydrous DMC, then were washed with acetone and dried overnight.

Electrochemical measurement

The working electrode was prepared by coating the N-methyl-2-pyrrolidone (NMP)-based slurry containing the as-prepared Li_2MnO_3 (or Co_3O_4@Li_2MnO_3), acetylene black and polyvinylidene difuoride (PVDF) in a weight ratio of 8 : 1 : 1 on aluminum foil (thickness: 20 μm) using a doctor-blade technique, and the coated foils were dried and punched into circular pieces (d =15 mm), which were further dried at 120 ^oC for 12 h under vacuum. The mass loading of Li_2MnO_3 (or Co_3O_4@Li_2MnO_3) was about 25 mg cm^{-2}. The Celgard 2730 membrane and LIB315 (a standard 1 mol L^{-1} $LiPF_6$ solution in a 1:1:1 mixture of ethylene carbonate, dimethyl carbonate, and diethyl carbonate, Guotaihuarong Chemical Plant) were used as the separator and the electrolyte, respectively. All cells were assembled in an Ar-filled glove box. The cyclic voltammetry was obtained between 2.0 and 5.0 V at a scan rate of 0.1 mV s^{-1} after the first charging process. The cycling tests were collected when the electrodes were first charged/discharged between 2.0 and 4.8 V and then charged/discharged between 2.0 and 4.6 V, and the current density is 10 mA g^{-1}.

3. Results and discussion

The preparation process of the core-shell structure of Co_3O_4@Li_2MnO_3 microsphere is shown in Scheme 1. At first, $MnCO_3$ microsphere was prepared by precipitation method and was used as the precursors for the further synthesis. The crystallinity of the precursor ($MnCO_3$ microsphere) is very high (Fig. S1a). Uniform microspheres with an average diameter of about 1.5 - 2.0 μm were obtained (Fig. S1b). Then LiOH was coated on the surface of $MnCO_3$ microspheres by a simple dipping-drying method. After that, this mixture was heat-treated and Li_2MnO_3 micropheres were

formed. Porous Co_3O_4 nanoparticles were coated on the Li_2MnO_3 microsphere by a hydrothermal method followed with a heat-treatment.

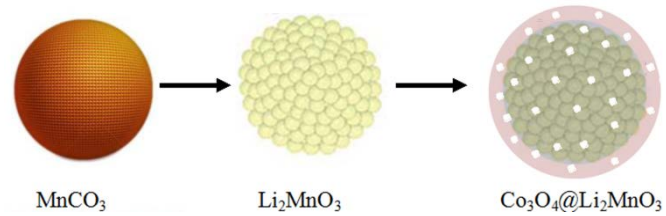

Scheme 1 The preparation process of the core-shell structure of Co_3O_4@Li_2MnO_3.

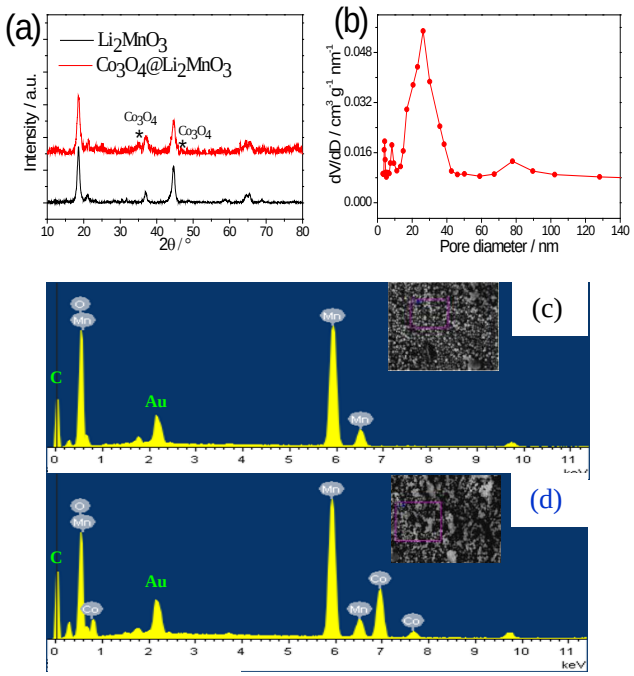

Fig.1 (a) XRD pattern of the Li_2MnO_3 microsphere and the core-shell Co_3O_4@Li_2MnO_3, (b) nitrogen adsorption–desorption isotherms (inset) and the Barrett–Joyner–Halenda (BJH) curve of the composite, energy dispersive X-ray spectroscopy (EDX) analysis for (c) the Li_2MnO_3 microsphere and (d) the core-shell Co_3O_4@Li_2MnO_3.

The XRD diffraction patterns of the Li_2MnO_3 and the composite (core-shell Co_3O_4@Li_2MnO_3) are shown in Fig. 1(a). All samples show a layered structure of the C2/m space group with alternating Li layers and transitional metal layers separated by oxygen layers. The superlattice peaks between 20 and 25° in the XRD, which are not observed in other layered materials, are due to the ordering of Li/Mn in the transitional metal layers.[18b] Minor amounts of Co_3O_4 phases are found from the XRD pattern of the composite.[18c] Nitrogen adsorption–desorption isotherm and the Barrett–Joyner–Halenda (BJH) curve for Co_3O_4@Li_2MnO_3 are shown in Fig. 1(b). The isotherm exhibits the type IV characteristics with a distinct hysteresis loop in the P/P_0 range of 0.45–1.0, which suggests the presence of nanopores.[19, 20] The pores with size of about 25 and 75 nm are resulted from the outer shell since the core does not show evidence of pores. The energy dispersive X-ray spectroscopy (EDS) analysis for the Co_3O_4@Li_2MnO_3 composite (Fig. 1d) presents the existence of Mn and Co besides Au and C signals from the sputtering prior to the measurement and FESEM grid and there is no Co signals for the Li_2MnO_3 (Fig. 1c). The amount of Co_3O_4 based on EDS analysis in the composite is 17.4 wt%.

Fig. 2 shows the SEM and TEM micrographs of the prepared Li_2MnO_3 microspheres and the core-shell composite. The low magnification SEM micrographs (Figs. 2a and 2b) reveal that the products are composed of microspheres with diameters of 1.5-2.0 μm. In the case of the Li_2MnO_3 microspheres, they are not porous. In contrast, the enlarged view of the Co_3O_4@Li_2MnO_3 microspheres indicates that some pores with an average size of between 20 nm to 80 nm exist on its surface, as shown in the inset of Fig. 2b, which is consistent with the above nitrogen absorption and desorption. It is clear that Co_3O_4 is uniformly coated on the surface of the Li_2MnO_3 microspheres, as shown in Fig.2d. The outer shell with porous feature is comprised of a large amount of interconnected Co_3O_4 nanoparticles (inset in Fig.2d). In addition, the micrometer-sized spherical Li_2MnO_3 can assure high tap density as well as high volumetric capacity. The average density of the as-prepared Li_2MnO_3 microspheres was determined to be 2.4 g cm^{-3}, while the density of as the Co_3O_4@Li_2MnO_3 was 2.0 g cm^{-3}. Of course, the porous structure of the shell is not beneficial to the increase of the density of the material. However, the pores from the outer shell (Co_3O_4) can provide pathways for the Li^+ ions into/out the inner core (Li_2MnO_3).

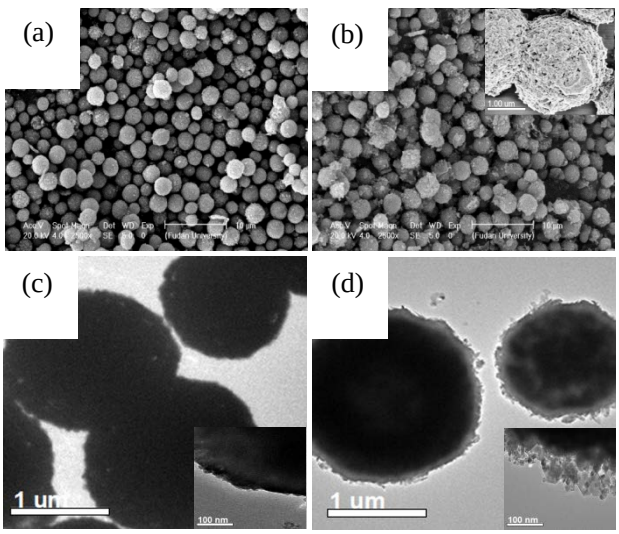

Fig. 2 SEM and FESEM (inset) micrographs of (a) the Li_2MnO_3 microsphere and (b) the core-shell Co_3O_4@Li_2MnO_3 composite, TEM micrographs of (c) the Li_2MnO_3 micropshere and (d) the core-shell Co_3O_4@Li_2MnO_3 composite.

The electrochemical properties of the Li_2MnO_3 microshere and the core-shell Co_3O_4@Li_2MnO_3 are shown in Fig. 3. The Li_2MnO_3 microsphere exhibits an initial charge and discharge capacities of

141 and 85 mAh g^{-1}, respectively. The voltage plateau above 4.5 V is connected with the removal of oxygen, which results in relative lower initial Coulombic efficiency.[10, 17] Such a phenomenon is commonly observed for Li_2MnO_3 and its related Li-rich layered materials.[10] It was reported that the activation of Li_2MnO_3 above 4.5 V led to the removal of O_2 molecules and the O_2 molecules were electrochemically reduced in the subsequent discharge.[17c] Very recently, direct observation of Li_2O evolution on Li-rich cathode material was achieved by using in situ surfaced-enhanced Raman spectroscopy (SERS).[17d] The core-shell of Co_3O_4@Li_2MnO_3 delivered an initial charge capacity as high as 183 mAh g^{-1} and discharge capacity of 178 mAh g^{-1}. The irreversible capacity loss of the core-shell of Co_3O_4@Li_2MnO_3 is basically eliminated. The discharge capacity of such a composite is higher than those of $LiCoO_2$,[21a,21b] $LiNi_{1/3}Co_{1/3}Mn_{1/3}O_2$, [19] and $LiFePO_4$,[21c] and also competitive with recently reported Ni-rich $Li[Ni_{1-x}M_x]O_2$ (M=transition metal) cathodes.[22] For cycling test, the first charge/discharge was carried in potential range of 2.0–4.8 V and the other cycles was in potential range of 2.0–4.6 V. As for the core-shell Co_3O_4@Li_2MnO_3 composite, after 50 cycles in this high voltage range, its discharge capacity maintains 135 mAh g^{-1}. The cycling behavior of the Co_3O_4@Li_2MnO_3 composite is better than that of the Li_2MnO_3 microspheres, which is due that the surface coating on Li-rich layered materials can protect the electrode from etching by acidic species in the electrolyte and suppress cathode corrosion/fragmentation, which is similar to the other coating.[15b]

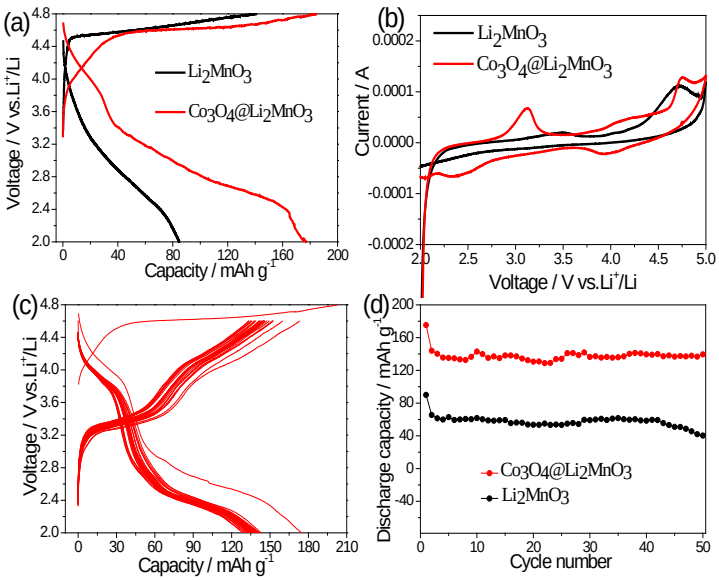

Fig. 3 Initial charge/discharge curves of (a) the Li_2MnO_3 microsphere and the core-shell Co_3O_4@Li_2MnO_3 composite, (b) the cyclic voltammograms of the Li_2MnO_3 and the Co_3O_4@Li_2MnO_3 between 2.0 and 5.0 V at a scan rate of 0.1 mV s^{-1} after the first charging process, (c) charge/discharge curves of Co_3O_4@Li_2MnO_3 during cycling, and (d) cycling behaviors of the Li_2MnO_3 microsphers and the core-shell Co_3O_4@Li_2MnO_3 composite.

Interestingly, from the charge/discharge curves of the composite (Fig. 3c), a charge plateau situated at 3.3 V and a discharge plateau at 2.4 V are observed, which are not observed in the charge/discharge curves of the virginal Li_2MnO_3. This is also consistent with the above CV curves of the Li_2MnO_3 microsphere and the core-shell Co_3O_4@Li_2MnO_3 (Fig. 3b). The ex-situ X-ray photoelectron spectroscopy (XPS) was used to investigate the surface electronic states of the Co_3O_4@Li_2MnO_3 electrodes. In Fig. S3, before cycling, the sample gives two main peaks at 779. 8 and 795.1 eV due to the $Co_{2p3/2}$ and $Co_{2p1/2}$, respectively, together with two satellite peaks at 788.6 and 803.7 eV, which are corresponding to Co-O bonds of Co_3O_4. [23a] However, when charged to 4.8 V, the binding energy peaks of Co_{2p} in the electrode shift slightly toward lower position which suggests that the outer shell react with something during this process. After discharged to 2.0 V, the binding energy peaks of Co_{2p} in the electrode shift slightly toward lower position. Then after 2nd charging to 4.8 V, the valence of cobalt increases, but the position of peaks is different from the state at the 1st charging to 4.8 V, which means that the reaction during the first charging to 4.8 V is irreversible. The XPS spectrum after 50 cycles is similar to the state at 1st discharging to 2.0 V. In a previous report, [23b] it was found that during the charging process, the Li_2O/CoO mixture can be oxidized into Co_3O_4, and then the Co_3O_4 can result in the formation of Li_xCoO_y in the higher-voltage region (above 4.2 V vs. Li^+/Li). Based on these analyses, it is speculated that, in our core-shell structured Co_3O_4@Li_2MnO_3 composite, the outer shell Co_3O_4 can react with the Li_2O during the first charging to high voltage. The charging process for the composite is suggested as equations (1):

$$Co_3O_4 + (3y\text{-}4)\ Li_2O \xrightarrow{\text{Charge}} 3Li_xCoO_y + (6y\text{-}3x\text{-}8)\ Li^+ + (6y\text{-}3x\text{-}8)e^- \quad (1)$$

Then during the following discharge to 2.0 V, according the changes in the valence of cobalt and the electrochemical data, the subsequent process is suggested as equations (2):

$$Li_xCoO_y + zLi^+ + ze^- \underset{\text{Charge}}{\overset{\text{Discharge}}{\Longleftrightarrow}} Li_{x+z}CoO_y \quad (2)$$

The relatively low initial Coulombic efficiency of Li_2MnO_3 is closely related to the irreversible lithium deintercalation/ intercalation. That is, the Li_2O (or Li^+ and O_2) were first removed from the Li_2MnO_3 during the activation process during the initial charging process, which yields a component MnO_2 that can only accommodate half of the extracted Li^+ ions during the discharging back to the rock-salt stoichiometry. Moreover, some oxygen may react with the electrolyte, which increases the irreversible capacity. However, in the core-shell Co_3O_4@Li_2MnO_3 composite, the coating layer (Co_3O_4) perhaps help to suppress oxygen emission of Li_2MnO_3 by absorbing the produced Li_2O (Li^+ and O_2) as the possible reaction (1). During the subsequent discharging/charging processes, the Li^+ ions can intercalate/ deintercalate into/from the Li_xCoO_y and the core (a component MnO_2 or $Li_{2-x}MnO_{3-x/2}$). The reaction (1) and the subsequent Li^+ ions deintercalation/intercalation from/into the Li_xCoO_y phase (reaction (2)) can be described as the synergistic effect between Li_2MnO_3 and Co_3O_4. Such synergistic effect successfully avoids the oxygen emission and decreases the initial irreversible capacity of Li_2MnO_3. Of course, further direct evidence about the no-emission of oxygen is needed in the future.

In addition, there is a couple of redox peaks suited at around 4.2 V (Fig. 3d), which is also observed at the charge/discharge curves (Fig. 3c). This is because that a small amount of Co ions incorporates into the layered oxide lattice during the heating process and minor $Li[Li_{(1-x)/3}Co_xMn_{(2-2x)/3}]O_2$ exists in the composite, which results in the weak redox peaks and the charge/discharge plateau at around 4.2 V.[24] Actually, previous work also show that annealing Li-rich materials modified by the $AlPO_4$ and Li-Ni-PO_4 at high temperatures lead to an incorporation of some Al^{3+} and Ni^{2+} into the layered oxide lattice and the formation of Li_3PO_4 on the surface.[13b,16]

According to such synergistic effect, the lower amount of Co_3O_4 coating will lead to the relative larger irreversible capacity loss of Li_2MnO_3. When the amount of Co_3O_4 coating increases from 4.7% to 10.1%, the irreversible capacity loss decreases from above 60 to only 30 mAh g^{-1} (Fig. S4). As Fig. 3 (c) shows the initial irreversible capacity is very few when the coating amount of Co_3O_4 is 17.4%. These results clearly indicate that the removed Li_2O in the initial activation charge process for Li_2MnO_3 is absorbed by the Co_3O_4 coating since there will be large irreversible capacity if the oxygen emission happens. Given the application of lithium ion battery, the existence of O_2 in the electrolyte is very dangerous and easily causes safety issue. A perhaps obvious appeal of our approach is that it might be extended to eliminate the irreversible capacities loss of solid solutions (such as xLi_2MnO_3•1-$xLiCoO_2$, xLi_2MnO_3•1-$xLiNi_{1/2}Mn_{1/2}O_2$, xLi_2MnO_3•1-$xLiCrO_2$ and xLi_2MnO_3•1-$xLiNi_{1/3}Co_{1/3}Mn_{1/3}O_2$).[12a,12b,17c,17d,25] Not only the huge irreversible capacity but also the release of O_2 in solid solutions can be suppressed by coating Co_3O_4 on its surface.

Conclusions

In summary, Li_2MnO_3 microsphere is prepared by a simple reaction of $MnCO_3$ microsphere with LiOH. Then a nanoporous Co_3O_4 is coated on the microsphere. The coating can eliminate the irreversible capacity loss and the possible release of O_2 or Li_2O in Li-rich materials. The cycling performance of such core–shell structure of porous Co_3O_4 grown on Li_2MnO_3 microsphere is good. The attraction of our porous Co_3O_4 coating approach is that it can be extended to other coating to eliminate the irreversible capacities loss of Li_2MnO_3 and its solid solutions with layered $LiMO_2$.

Acknowledgements

Financial support from Distinguished Young Scientists Program of NSFC (51425301) and Showa Denko Company is greatly appreciated.

Notes and references

[a] College of Energy, Nanjing Tech University, Nanjing 211816, Jiangsu Province, China
E-mail: zhuys01@126.com
[b] New Energy and Materials Laboratory (NEML), Department of Chemistry & Shanghai Key Laboratory of Molecular Catalysis and Innovative Materials, Fudan University, Shanghai 200433, China.
E-mail: wuyp@fudan.edu.cn; Fax: + 86-21-55664223

Electronic Supplementary Information (ESI) available: XRD pattern, SEM and FESEM micrographs of $MnCO_3$, nitrogen adsorption-desorption isotherm, XPS spectra of the composite electrodes conducted to the different charge/discharge state and charge/discharge curves of Li_2MnO_3 coated by Co_3O_4 with low concentration. See DOI: 10.1039/b000000x/

1. (a) H. B. Wu, J. S. Chen, X. W. Lou and H. H. Hng, *J. Phys. Chem. C* 2011, **115**, 24605; (b) G. J. Wang, L. J. Fu, N. H. Zhao, L. C. Yang, Y. P. Wu and H. Q. Wu, *Angew. Chem., Int . Ed.*, 2007, **46**, 295; (c) N. H. Zhao, G. J. Wang, Y. Huang, B. Wang, B. D. Yao and Y. P. Wu, *Chem. Mater.*, 2008, **20**, 2612; (d) Y. S. Zhu, F. X. Wang, L. L. Liu, S. Y. Xiao, Z. Chang and Y. P. Wu, *Energy Environ. Sci.*, 2013, **6**, 618; (e) W. Tang, Y. Hou, F. Wang, L. Liu, Y. Wu and K. Zhu, *Nano Lett.*, 2013, **13**, 2036; (f) Y. S. Zhu, F. X. Wang, L. L. Liu, S. Y. Xiao, Y. Q. Yang and Y. P. Wu, *Sci. Rep.*, 2013, **3**, 3187; (g) S. Ding and X. W. Lou, *Nanoscale*, 2011, **3**, 3586.
2. (a) X. L. Xiao, J. Lu, and Y. D. Li, *Nano Res.*, 2010, **3**, 733; (b) S. M. Oh, S. T. Myung, Y. S. Choi, K. H. Ohd and Y. K. Sun, *J. Mater. Chem.*, 2011, **21**, 19368; (c) H. G. Jung, S. T. Myung, C. S. Yoon, S. B. Son, K. H. Oh, K. Amine, B. Scrosati and Y. K. Sun, *Energy Environ. Sci.*, 2011, **4**, 1345; (d) V. G. Pol and M. M. Thackeray, *Energy Environ. Sci.*, 2011, **4**, 1904.
3. (a) X. Lai, J. E. Halpert and D. Wang, *Energy Environ. Sci.*, 2012, **5**, 5604. (b) H. Wu, G. Chan, J. W. Choi, I. Ryu, Y. Yao, M. T. McDowell , S. W. Lee, A. Jackson, Y. Yang, L. Hu and Y. Cui, *Nat. Nanotechnol.* , **7**, 310; (c) X. L. Wang, M. Feygenson, H. Chen, C. H. Lin, W. Ku, J. Bai, M. C. Aronson, T. A. Tyson and W. Q. Han, *J. Am. Chem. Soc.*, 2011, **133**, 11213; (d) J. Du, J. Qi, D. Wang and Z. Tang, *Energy Environ. Sci.*, 2012, **5**, 6914; (e) S. M. Oh, S. T. Myung, J. B. Park, B. Scrosati, K. Amine and Y. K. Sun, *Angew. Chem., Int. Ed.*, 2012, **51**, 1853; (f) L. He, Z. M. Liao, H. C. Wu, X. X. Tian, D. S. Xu, G. L. Cross, G. S. Duesberg, I. V. Shvets and D. P. Yu, *Nano Lett.*, 2011, **11**, 4601.
4. (a) J. Yan, A. Sumboja, E. Khoo and P. S. Lee, *Adv. Mater.*, 2011, **23**, 746; (b) X. Chen, X. Li, F. Ding, W. Xu, J. Xiao, Y. Cao, P. Meduri, J. Liu, G. L. Graff and J. G. Zhang, *Nano Lett.*, 2012, **12**, 4124; (c) B. Luo, B. Wang, M. Liang, J. Ning, X. Li and L. Zhi, *Adv. Mater.*, 2012, **24**, 1405.
5. (a) Q. Qu, Y. Zhu, X. Gao and Y. Wu, *Adv. Energy Mater.*, 2012, **2**, 950; (b) W. Tang, L. Liu, Y. Zhu, H. Sun, Y. Wu and K. Zhu, *Energy Environ. Sci.*, 2012, **5**, 6909; (c) W. Tang, Y. Zhu, Y. Hou, L. Liu, Y. Wu, K. P. Loh, H. Zhang and K. Zhu, *Energy Environ. Sci.*, 2013, **6**, 2093; (d) C. Zhang, H. B. Wu, C. Yuan, Z. Guo and X. W. Lou, *Angew. Chem., Int. Ed.*, 2012, **51**, 9592; (e) D. J. Xue, S. Xin, Y. Yan, K. C. Jiang, Y. X. Yin, Y. G. Guo and L. J. Wan, *J. Am. Chem. Soc.*, 2012, **134**, 2512; (f) L. Q. Mai, F. Yang, Y. L. Zhao, X. Xu, L. Xu, Y. Z. Luo, *Nat. Commun.*, 2011, **2**, 381.
6. (a) M. M. Thackeray, S.-H. Kang, C. S. Johnson, J. T. Vaughey, R. Benedek and S. A. Hackney, *J. Mater. Chem.*, 2007, **17**, 3112; (b) W. P. Tang, *Chem. Mater.*, 2000, **12**, 3271.
7. (a) A. D. Robertson and P. G. Bruce, *Chem. Commun.*, 2002, 2790; (b) A. D. Robertson and P. G. Bruce, *Chem. Mater.*, 2003, **15**, 1984.
8. (a) D. Pasero, V. McLaren, S. Souza and A. R. West, *Chem. Mater.*, 2005, **17**, 345; (b) J. Y. Baek, H. W. Ha, I. Y. Kim and S. J. Hwang, *J. Phys. Chem. C*, 2009, **113**, 17392.

9. (a) J. R. Croy, D. Kim, M. Balasubramanian, K. Gallagher, S.-H. Kang and M. M. Thackeray, *J. Electrochem. Soc*., 2012, **159**, A781; (b) D. Y. W. Yu, K. Yanagida, Y. Kato and H. Nakamura, *J. Electrochem. Soc.*, 2009, **156**, A417.
10. (a) J. Lim, J. Moon, J. Gim, S. Kim, K. Kim, J. Song, J. Kang, W. B. Im and J. Kim, *J. Mater. Chem.*, 2012, **22**, 11772; (b) Y. N. Ko, J. H. Kim, J. K. Lee, Y. C. Kang, J. H. Lee, *Electrochim. Acta*, 2012, **69**, 345; (c) X. K. Zhang, S. L. Tang, Y. W. Du, *Mater. Res. Bull.*, 2012, **47**, 636; (d) J. Gim, J. Song, H. Park, J. Kang, K. Kim, V. Mathew and J. Kim, *Nanoscale Res. Lett.*, 2012, 7, 60.
11. B. Xu, C. R. Fell, M. Chi and Y. S. Meng, *Energy Environ. Sci.*, 2011, **4**, 2223.
12. (a) F. Wu, N. Li, Y. Su, H. Shou, L. Bao, W. Yang, L. Zhang, R. An and S. Chen, *Adv. Mater.* , 2013, **25**, 3722; (b) M. Gu, I. Belharouak, J. Zheng, H. Wu, J. Xiao, A. Genc, K. Amine, S. Thevuthasan, D. R. Baer, J. G. Zhang, N. D. Browning, J. Liu and C. Wang, *ACS Nano*, 2013, **7**, 760; (c) F. X. Wang, S. Y. Xiao, Z. Chang, M. X. Li, Y. P. Wu, R. Holze, *Int. J. Electrochem. Sci.*, 2014, **9**, 6182.
13. (a) S. H. Kang and M. M. Thackeray, *Electrochem. Commun.*, 2009, **11**, 748; (b) D. Shin, C. Wolverton, J. R. Croy, M. Balasubramanian, S. H. Kang, C. M. L. Rivera and M. M. Thackeray, *J. Electrochem. Soc*., 2012, **159**, A121.
14. (a) Y. J. Liu, S. B. Liu, Y. P. Wang, L. Chen and X. H. Chen, *J. Power Sources*, 2013, **222**, 455; (b) J. M. Zheng, Z. R. Zhang, X. B. Wu, Z. X. Dong, Z. Zhu and Y. Yang, *J. Electrochem. Soc*., 2008, **155**, A775.
15. (a) Y. K. Sun, M. J. Lee, C. S. Yoon, J. Hassoun, K. Amine and B. Scrosati, *Adv. Mater*., 2012, **24**, 1192; (b) J. Zheng, M. Gu, J. Xiao, P. Zuo, C. Wang and J. G. Zhang, *Nano Lett.*, 2013, **13**, 3824.
16. Y. Wu, A. Vadivel Murugan and A. Manthiram, *J. Electrochem. Soc*., 2008, **155**, A635.
17. (a) G. Singh, R. Thomas, A. Kumar, R. S. Katiyar and A. Manivannan, *J. Electrochem. Soc*., 2012, **159**, A470; (b) Y. Wu and A . Manthiram, *Solid State Ionics*, 2009, **180**, 50; (c) N. Yabuuchi, K. Yoshii, S. T. Myung, I. Nakai and S. Komaba, *J. Am. Chem. Soc*., 2011, **133**, 4404; (d) S. Hy, F. Felix, J. Rick, W. N. Su and B. J. Hwang, *J. Am. Chem. Soc*., 2014, **136**, 999.
18. (a) L. Zhou, D. Zhao, and X. W. Lou, *Angew. Chem. Int. Ed.*, 2012 , **51** , 239. (b) G. Singh, R. Thomas, A. Kumar and R. S. Katiyar, *J. Electrochem. Soc*., 2012, **159**, A410; (c) X. Xiao, X. Liu, H. Zhao, D. Chen, F. Liu, J. Xiang, Z. Hu and Y. Li, *Adv. Mater*., 2012, **24**, 5762.
19. (a) F. Wang, S. Xiao, Z. Chang, Y. Yang and Y. Wu, *Chem. Commun.*, 2013, **49**, 9209; (b) L. Liu, Y. Hou, S. Xiao, Z. Chang, Y. Yang and Y. Wu, *Chem. Commun.*, 2013, 49, 11515.
20. (a) F. X. Wang, S. Y. Xiao, Y. S. Zhu, Z. Chang, C. L. Hu, Y. P. Wu and R. Holze, *J. Power Sources*, 2014, **246**, 19; (b) F. Wang, S. Xiao, X. Gao, Y. Zhu, H. Zhang,Y.Wu, R. Holze, *J. Power Sources*, 2013, **242**, 560.
21. (a) S. Luo, K. Wang, J. Wang, K. Jiang, Q. Li and S. Fan, *Adv. Mater*., 2012, **24**, 2294; (b) W. Tang, L.L. Liu, S. Tian, L.Li, Y.B. Yue, Y.P. Wu , S.Y. Guan, K. Zhu, *Electrochem. Commun*., 2010, **12**, 1524; (c)Y. Y. Hou, X. J. Wang, Y. S. Zhu, C.L. Hu, Z. Chang, Y. P. Wu and R. Holze, *J. Mater. Chem. A* , 2013, **1** , 14713.
22. (a) Y. K. Sun, Z. Chen, H. J. Noh, D. J. Lee, H. G. Jung, Y. Ren, S. Wang, C. S. Yoon, S. T. Myung and K. Amine, *Nat. Mater*., 2012, **11**, 942; (b) H. J. Noh, S. T. Myung, H. G. Jung, H. Yashiro, K. Amine and Y. K. Sun, *Adv. Funct. Mater.*, 2013, **23**, 1028.
23. (a) L. Tao, J. Zai, K. Wang, H. Zhang, M. Xu, J. Shen, Y. Su, X. F. Qian. J. Power Sources, 2012, 202, 230; (b) J. Shu, M. Shui, F. Huang, Y. Ren, Q. Wang, D. Xu and L. Hou, *J. Phys. Chem. C* 2010, **114**, 3323.
24. (a) J. M. Kim, S. Tsuruta and N. Kumagai, *Electrochem. Commun*., 2007, **9**, 103; (b) J. Bareno, M. Balasubramanian, S. H. Kang, J. G. Wen, C. H. Lei, S. V. Pol, I. Petrov and D. P. Abraham, *Chem. Mater*., 2011, **23**, 2039.
25. (a) Y. Liu, S. Liu, Y. Wang, L. Chen and X. Chen, *J. Power Sources*, 2013, **222** , 455; (b) Y. Lee, M. Kim and J. Cho, *Nano Lett.*, 2008, **8**, 957; (c) A. Boulineau, L. Simonin, J. F. Colin, C. Bourbon and S. Patoux, *Nano Lett.*, 2013, **13**, 3857.

